MORTAR FINITE ELEMENTS FOR INTERFACE PROBLEMS

BISHNU P. LAMICHHANE* AND BARBARA I. WOHLMUTH*

Abstract. Mortar techniques provide a flexible tool for the coupling of different discretization schemes or triangulations. Here, we consider interface problems within the framework of mortar finite element methods. We start with a saddle point formulation and show that the interface conditions enter into the right-hand side. Using dual Lagrange multipliers, we can work with scaled sparse matrices, and static condensation gives rise to a symmetric and positive definite system on the unconstrained product space. The iterative solver is based on a modified multigrid approach. Numerical results illustrate the performance of our approach.

Key words. Mortar finite elements, Lagrange multiplier, saddle point problem, domain decomposition, interface problem, non-matching triangulation

AMS subject classifications. 65N30, 65N55

1. Introduction. Domain decomposition techniques provide powerful tools for the coupling of different discretization schemes or of non-matching triangulations. Non-matching triangulations are of interest, for example, if different subdomains are meshed independently, or if adaptive remeshing is done in some subdomains. This can be caused by discontinuous diffusion coefficients, problems with transmission conditions at the interface, local anisotropies, singular sources or corner singularities. Here, we consider mortar finite elements for interface problems. Such interface problems arise in different situations, for example, in heat conduction or in linear elasticity. The characteristic idea of mortar methods is to decompose the domain of interest in non-overlapping subdomains and to replace the strong pointwise continuity at the interfaces by a weak integral condition. There are two different equivalent variational formulations. One approach results in a positive definite system on the constrained mortar space [BMP93, BMP94], and a second one gives rise to an indefinite system associated with the unconstrained product space and a Lagrange multiplier space [Bel99]. Here, we follow the second approach and rewrite the interface problem as indefinite variational equation.

Conforming finite element methods for elliptic problems with discontinuous coefficients and homogeneous interface conditions are addressed in [Bab70]. Finite element methods for non-homogeneous elliptic interface problems are analyzed in [BK96], and it is shown that the discretization error is of optimal order for linear finite elements on quasi-uniform triangulations. A survey on non-overlapping domain decomposition methods for elliptic interface problems can be found in [XZ98]. A least-squares finite element method for elliptic interface problems with Dirichlet and Neumann boundary data is proposed and analyzed in [CG98]. In particular, error estimates for non-matching triangulations at the interface are given. Elliptic and parabolic interface problems with a non-zero jump in the flux across a sufficiently smooth interface are considered in [CZ98, HZ02]. In [CZ98], nearly optimal error estimates in the energy-norm and in the L^2-norm are established under reasonable regularity assumptions on the original solutions, whereas some new a priori estimates are presented in [HZ02].

*IANS, University of Stuttgart, Germany. {lamichhane,wohlmuth}@mathematik.uni-stuttgart.de.
This work was supported in part by the Deutsche Forschungsgemeinschaft, SFB 404, C12.

The immersed interface method is based on using the jumps in the solution and its derivative to modify standard finite difference schemes in the neighborhood of the interface, see [LL94]. The idea to precondition the elliptic equation before using the immersed interface method is proposed in [Li98a] resulting in a fast algorithm for elliptic equations with large jumps in the coefficients. An extension of the immersed interface method to boundary value problems on irregular domains with Neumann and Dirichlet boundary conditions can be found in [WB00]. The immersed interface method with a finite element formulation is considered in [Li98b]. Nitsche techniques provide flexible domain decomposition techniques and have been successfully used for the numerical approximation of partial differential equations, see, e.g., [BHS03, HN03]. The analysis of the discretization scheme is restricted to homogeneous interface conditions, and optimal a priori estimates are given. A similar approach can be found in [HH02], where a stationary heat conduction problem in two dimensions with a discontinuous conducting coefficient across a smooth interface is considered. Optimal a priori estimates for appropriately modified piecewise linear elements on a quasi-uniform triangulation have been established. Mortar methods based on dual Lagrange multiplier spaces for elliptic problems are considered in [Woh01]. Here, we propose a similar approach based on mortar techniques and dual Lagrange multipliers. We consider non-homogeneous jumps in the flux and in the solution across the interface. Starting with a saddle point formulation of the interface problem, we show the existence and uniqueness of the solution in the continuous and discrete setting. In contrast to the general mortar framework, we decompose the interface into disjoint straight lines and remove a degree of freedom of Lagrange multipliers from its corner nodes. We show that this is essential to prove an optimal a priori estimate for the piecewise linear interface. Compared to standard formulations for the Laplace operator, see [BMP93], we have to include two additional terms reflecting the interface conditions. The jump terms enter only in the right-hand side, and the arising stiffness matrix does not depend on the interface conditions. Working with dual Lagrange multiplier spaces, a flexible and efficient coupling of non-matching triangulations at the interface can be realized. In terms of the biorthogonality between the basis functions of the finite element trace and the Lagrange multiplier space, we get a diagonal mass matrix on the slave side. As a consequence, we can locally eliminate the Lagrange multiplier from the saddle point formulation and obtain a positive definite algebraic system on the unconstrained product space. Hence, the multigrid method introduced in [WK01] can be applied to our situation. Our approach is quite flexible and can easily be applied to general type of elliptic and parabolic interface problems, where the geometry of and the jump at the interface are a priori known.

The paper is organized as follows: In the next section, we present our model interface problem and introduce its saddle point formulation in the continuous setting. In Section 3, we briefly outline the mortar discretization scheme and establish a priori estimates for the discretization errors. Moreover, we consider the algebraic formulation of the saddle point problem. Local modifications are carried out to obtain a positive definite system for which we can use multigrid methods. Finally in Section 4, we show some numerical results illustrating the performance of our approach. In particular, we give the discretization errors in the L^2- and H^1-norm and in a weighted L^2-norm for the Lagrange multiplier.

2. Continuous setting. Let us consider a bounded polygonal domain $\Omega \subset \mathbb{R}^2$, which is decomposed into two non-overlapping subdomains Ω_1 and Ω_2 with the common interior interface Γ, $\bar{\Gamma} := \partial\Omega_1 \cap \partial\Omega_2$, and assume that the interface Γ can be written as union of straight lines, see Figure 2.1. For simplicity, we restrict ourselves to the case of two subdomains. However, the approach can be generalized to more than two subdomains. We

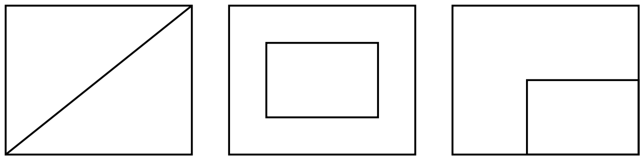

Fig. 2.1: Different decompositions of the domain into two subdomains

consider the following elliptic second order boundary value problem on Ω

$$-\mathrm{div}(\alpha_i \nabla u_i) + b_i u_i = f_i \quad \text{in} \quad \Omega_i, \quad i = 1,2 \tag{2.1}$$

with homogeneous Dirichlet boundary conditions on $\partial\Omega$. Here, α_1 and α_2 are symmetric and locally constant positive-definite second order tensors specifying the diffusion in the two subdomains. Furthermore, we assume that $f_i \in L^2(\Omega_i)$ and $0 \leq b_i \in L^\infty(\Omega_i), i = 1,2$. The jump conditions at the interface Γ are given by

$$[u] := u_1 - u_2 = g_D \quad \text{on} \quad \Gamma, \tag{2.2}$$

$$[u]_n := (\alpha_1 \nabla u_1) \cdot n_1 + (\alpha_2 \nabla u_2) \cdot n_2 = g_N \quad \text{on} \quad \Gamma, \tag{2.3}$$

where n_i is the outward normal on $\partial\Omega_i$. We assume that $g_D \in H_{00}^{\frac{1}{2}}(\Gamma)$ and $g_N \in H^{-\frac{1}{2}}(\Gamma) := \left(H_{00}^{\frac{1}{2}}(\Gamma)\right)'$. On each subdomain, we define

$$H_*^1(\Omega_k) := \{v \in H^1(\Omega_k), v_{|\partial\Omega\cap\partial\Omega_k} = 0\}, \quad k = 1,2,$$

and we work with the unconstrained product space $X := H_*^1(\Omega_1) \times H_*^1(\Omega_2)$.

Using a discretization scheme, we cannot, in general, satisfy the interface conditions (2.2) and (2.3) in a strong form. We replace (2.2) and (2.3) by a weak variational condition. It is given in terms of the duality pairing on the interface

$$b(v,\mu) := \langle [v], \mu \rangle_\Gamma, \quad v = (v_1, v_2) \in X, \quad \mu \in M := H^{-\frac{1}{2}}(\Gamma).$$

In the rest of this section, we consider the variational formulation of the interface problem. The weak formulation of (2.1) is obtained by applying Green's formula on Ω_i, $i = 1,2$

$$\int_{\Omega_i} (\alpha_i \nabla u_i) \cdot \nabla \phi_i \, dx - \int_\Gamma \alpha_i \nabla u_i \cdot n_i \phi_i \, ds + \int_{\Omega_i} b_i u_i \phi_i \, dx = \int_{\Omega_i} f_i \phi_i \, dx, \quad \phi_i \in H_*^1(\Omega_i).$$

Taking into account the interface condition for the flux (2.3), $\alpha_1 \nabla u_1 \cdot n_1 = -\alpha_2 \nabla u_2 \cdot n_2 + g_N$ on Γ, we find for $\phi_1 \in H_*^1(\Omega_1)$

$$\int_{\Omega_1} (\alpha_1 \nabla u_1) \cdot \nabla \phi_1 \, dx + \int_\Gamma \alpha_2 \nabla u_2 \cdot n_2 \phi_1 \, ds + \int_{\Omega_1} b_1 u_1 \phi_1 \, dx = \int_{\Omega_1} f_1 \phi_1 \, dx + \int_\Gamma g_N \phi_1 \, ds.$$

The weak formulation of the jump of the solution at the interface can be obtained by multiplying the jump condition (2.2) with an element of the dual space M. Then the definition of the bilinear form $b(\cdot,\cdot)$ yields

$$b(u,\mu) = \langle g_D, \mu \rangle_\Gamma =: g(\mu), \quad \mu \in M.$$

Introducing the flux $\lambda := \alpha_2 \nabla u_2 \cdot n_2$ on Γ, we can write the weak form of (2.1) as a saddle point problem: find $(u, \lambda) \in X \times M$ such that

$$\begin{array}{rcll} a(u,v) + b(v,\lambda) & = & f(v), & v \in X, \\ b(u,\mu) & = & g(\mu), & \mu \in M, \end{array} \tag{2.4}$$

where

$$a(u,v) := \sum_{k=1}^{2} \int_{\Omega_k} (\alpha_k \nabla u) \cdot \nabla v + b_k uv \, dx, \quad f(v) := \sum_{k=1}^{2} \int_{\Omega_k} f_k v \, dx + \left\langle v_{|\partial\Omega_1}, g_N \right\rangle_\Gamma .$$

The essential points for the existence and the uniqueness of the solution of a saddle point problem are coercivity, continuity and a suitable inf-sup condition. On X, we use the broken H^1-norm

$$\|v\|_{1,\Omega}^2 := \|v\|_{1,\Omega_1}^2 + \|v\|_{1,\Omega_2}^2,$$

and on M the $H^{-\frac{1}{2}}$-norm. We start with the continuity of the bilinear form $b(\cdot,\cdot)$. By definition, we find

$$b(v,\mu) = \langle [v], \mu \rangle_\Gamma \leq \|[v]\|_{H_{00}^{\frac{1}{2}}(\Gamma)} \|\mu\|_{H^{-\frac{1}{2}}(\Gamma)}, \quad v \in X, \, \mu \in M.$$

We note that if Γ is a closed curve, see the middle picture of Figure 2.1, we have $H_{00}^{\frac{1}{2}}(\Gamma) = H^{\frac{1}{2}}(\Gamma)$, and thus

$$\|[v]\|_{H_{00}^{\frac{1}{2}}(\Gamma)} = \|[v]\|_{H^{\frac{1}{2}}(\Gamma)} \leq (\|v_{|\Omega_1}\|_{H^{\frac{1}{2}}(\Gamma)} + \|v_{|\Omega_2}\|_{H^{\frac{1}{2}}(\Gamma)}) \leq C \|v\|_{1,\Omega}, \quad v \in X.$$

Due to the homogeneous Dirichlet boundary condition imposed on $\partial\Omega$, we find $(v_{|\Omega_i})_{|\Gamma} \in H_{00}^{\frac{1}{2}}(\Gamma)$, $i = 1, 2$, if Γ is not a closed curve. In that case, we can bound

$$\|[v]\|_{H_{00}^{\frac{1}{2}}(\Gamma)} \leq C (\|v_{|\Omega_1}\|_{H^{\frac{1}{2}}(\partial\Omega_1)} + \|v_{|\Omega_2}\|_{H^{\frac{1}{2}}(\partial\Omega_2)}) \leq C \|v\|_{1,\Omega}, \quad v \in X.$$

As a consequence, we obtain the continuity of the bilinear form $b(\cdot,\cdot)$ on $X \times M$. The bilinear form $a(\cdot,\cdot)$ is continuous on $X \times X$ and coercive on $Y \times Y$, where $Y := \{v \in X, \int_\Gamma [v] ds = 0\}$, [BMP93]. To see that the inf-sup condition holds, we start with the definition of the dual norm

$$\|\mu\|_{H^{-\frac{1}{2}}(\Gamma)} := \sup_{v \in H_{00}^{\frac{1}{2}}(\Gamma) \setminus \{0\}} \frac{\langle v, \mu \rangle_\Gamma}{\|v\|_{H_{00}^{\frac{1}{2}}(\Gamma)}} = \sup_{v \in H_{00}^{\frac{1}{2}}(\Gamma) \setminus \{0\}} \frac{b(\tilde{v}, \mu)}{\|v\|_{H_{00}^{\frac{1}{2}}(\Gamma)}} \leq C \sup_{v \in X \setminus \{0\}} \frac{b(v,\mu)}{\|v\|_{1,\Omega}},$$

where $\tilde{v}$ denotes the harmonic extension of v to Ω_2 extended by zero on Ω_1. Hence, the variational problem (2.4) has a unique solution.

3. Mortar discretizations and a priori error estimates. In this section, we briefly review mortar finite elements and prove optimal a priori estimates for the discretization errors. Let $\mathcal{T}_{h_1}$ and $\mathcal{T}_{h_2}$ be independent shape regular simplicial triangulations on Ω_1 and Ω_2 with meshsizes bounded by h_1 and h_2, respectively. Without loss of generality, the interface Γ inherits its one-dimensional mesh from $\mathcal{T}_{h_2}$. The side of Γ associated with Ω_2 is called slave side and the one associated with Ω_1 master side. We denote by $\mathcal{T}_\Gamma$ the triangulation on Γ with meshsize bounded by h_2 whose elements are boundary edges of $\mathcal{T}_{h_2}$. The unconstrained discrete finite element space is denoted by

$$X_h := \mathcal{S}^p(\Omega_1, \mathcal{T}_{h_1}) \times \mathcal{S}^p(\Omega_2, \mathcal{T}_{h_2}),$$

where $\mathcal{S}^p(\Omega_k, \mathcal{T}_{h_k})$ stands for the space of linear ($p = 1$) or quadratic ($p = 2$) conforming finite elements in the subdomain Ω_k associated with the triangulation $\mathcal{T}_{h_k}$ and satisfies homogeneous Dirichlet boundary conditions on $\partial\Omega_k \cap \partial\Omega$, $k = 1, 2$. We note that no interface condition is imposed on X_h, and the elements in X_h do not have to satisfy a continuity condition at the interface. Let W_h be the trace space of finite element basis functions from the slave side, i.e., of $S^p(\Omega_2, \mathcal{T}_{h_2})$, restricted to Γ. Due to the homogeneous boundary conditions on $\partial\Omega$, we find $W_h \subset H_{00}^{\frac{1}{2}}(\Gamma)$. To satisfy a suitable discrete inf-sup condition, we use a discrete Lagrange multiplier space such that $\dim M_h \leq \dim W_h$. A natural and efficient choice for the construction of a good Lagrange multiplier space is to define its basis functions locally and to associate them with the interior nodes of the slave side. Under the regularity assumption $u \in H^{p+1}(\Omega_2)$, λ is, in general, not an element in $H^{p-\frac{1}{2}}(\Gamma)$. This is due to the fact that the normal has jumps if Γ has corners. Therefore, we decompose Γ into a finite number of disjoint straight segments γ_l, $1 \leq l \leq N$, of maximal length, i.e., $\bar{\Gamma} = \cup_{l=1}^N \bar{\gamma}_l$, $\gamma_k \cap \gamma_l = \emptyset$, $l \neq k$ and $\bar{\gamma}_k \cup \bar{\gamma}_l$ is not a straight line, $1 \leq k \neq l \leq N$. In the examples given in Figure 2.1, we find $N = 1$, $N = 4$, and $N = 2$ (from the left to the right). We now work with the Lagrange multiplier spaces defined on γ_l. We remark that we use the decomposition of Γ into straight lines for the definition of the discrete Lagrange multiplier space, but that we work with the $H_{00}^{\frac{1}{2}}$-norm on Γ. Now, we denote by $W_h(\gamma_l)$, the trace of $S^p(\Omega_2, \mathcal{T}_{h_2})$ restricted to γ_l, and we set $W_{0;h}(\gamma_l) := H_0^1(\gamma_l) \cap W_h(\gamma_l)$. Our discrete Lagrange multiplier space is defined as the product space

$$M_h := \prod_{l=1}^{N} M_h(\gamma_l),$$

where $\dim M_h(\gamma_l) = \dim W_{0;h}(\gamma_l)$. Let us denote the nodal basis functions in $W_{0;h}(\gamma_l)$, associated with the one-dimensional mesh on the slave side by $\{\varphi_i^l\}_{1\leq i \leq n_s^l}$, $n_s^l := \dim W_{0;h}(\gamma_l)$. We use dual Lagrange multiplier spaces defined in [Woh01]. Then, the basis functions $\{\mu_i^l\}_{1\leq i\leq n_s^l}$ of $M_h(\gamma_l)$ satisfy the following biorthogonality relation

$$\int_{\gamma_l} \mu_i^l \, \varphi_j^l \, ds = \delta_{ij} \int_{\gamma_l} \varphi_j^l \, ds \ , \quad 1 \leq i, j \leq n_s^l,$$

and we have $\sum_{i=1}^{n_s^l} \mu_i^l = 1$ on γ_l. Furthermore for $p = 2$, the linear hat functions are contained in the Lagrange multiplier space.

To establish a priori estimates for the discretization errors, we consider the saddle point formulation (2.4) of the interface problem and apply the theory of mixed finite elements. Replacing the space $X \times M$ by our discrete space $X_h \times M_h$ in (2.4), we obtain our discrete variational problem: find $(u_h, \lambda_h) \in X_h \times M_h$ such that

$$\begin{array}{rcll} a(u_h, v) \, + \, b(v, \lambda_h) & = & f(v), & v \in X_h, \\ b(u_h, \mu) & = & g(\mu), & \mu \in M_h. \end{array} \tag{3.1}$$

Since $X_h \subset X$ and $M_h \subset M$, we get the continuity of the bilinear form $a(\cdot, \cdot)$ on $X_h \times X_h$ and of $b(\cdot, \cdot)$ on $X_h \times M_h$. Observing $(\ker B)_h := \{v_h \in X_h | \quad b(v_h, \mu) = 0, \, \mu \in M_h\} \subset Y$, we obtain the coercivity of $a(\cdot,\cdot)$ on $(\ker B)_h \times (\ker B)_h$. In the following, the set of endpoints of γ_k in Ω, $1 \le k \le N$, will be denoted by

$$\mathcal{N}_c := \bigcup_{k \neq l} (\bar{\gamma}_k \cap \bar{\gamma}_l).$$

To establish the discrete inf-sup condition, we introduce $\tilde{W}_h \subset W_h$ with $\dim \tilde{W}_h = \dim M_h$ and assume that $\dim M_h(\gamma_k) \ge 2$, $1 \le k \le N$. We remark that $H^{-\frac{1}{2}}(\Gamma)$ is a stronger norm than the product norm on $\prod_{l=1}^N H^{-\frac{1}{2}}(\gamma_l)$, and therefore, we cannot work with $\prod_{l=1}^N W_{0;h}(\gamma_l)$ to get an uniform inf-sup condition. The basis functions $\tilde{\varphi}_i$ of $\tilde{W}_h$ are associated with the interior nodes of γ_l. If x_i is a node adjacent to an endpoint $x_j \in \Omega$ of some γ_l, we define $\tilde{\varphi}_i := \varphi_i + 0.5\varphi_j$, where φ_i denotes the standard nodal basis function of W_h, and for all other nodes, we set $\tilde{\varphi}_i := \varphi_i$. We note that only the basis functions associated with a node adjacent to a corner are modified and that the space $\tilde{W}_h$ has the standard approximation properties. The basis functions of $\tilde{W}_h$ in the linear case are shown in the left picture of Figure 3.1, and the dual Lagrange multiplier basis functions are shown in the right picture.

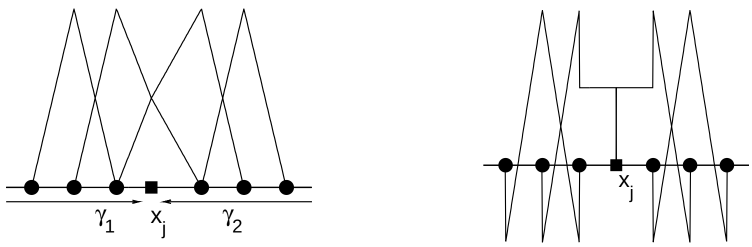

Fig. 3.1: Basis functions of $\tilde{W}_h$ (left) and of M_h (right), the basis functions are associated with the filled circles and x_j is a corner

Now, we define a projection operator Q_h by

$$Q_h : L^2(\Gamma) \longrightarrow \tilde{W}_h, \qquad \textstyle\int_\Gamma Q_h v\, \mu_h\, ds = \int_\Gamma v\, \mu_h\, ds, \qquad \mu_h \in M_h.$$

The biorthogonality of $M_h(\gamma_l)$ and $W_{0;h}(\gamma_l)$ and the modification of $\tilde{\varphi}_i$ at the nodes adjacent to endpoints of γ_l yield

$$\int_\Gamma \tilde{\varphi}_i \mu_k\, ds = \delta_{ik} \int_\Gamma \varphi_i\, ds + \sum_{x_j \in \mathcal{N}_c} \frac{c_{ij}}{2} \int_\Gamma \varphi_j \mu_k\, ds,$$

where $c_{ij} = 1$ if the node x_i is adjacent to the endpoint x_j and otherwise $c_{ij} = 0$. It can be easily verified that Q_h is well-defined. The structure of the mass matrices guarantees that the action of Q_h can be computed locally. Moreover, it is easy to see that $Q_h v = v$, $v \in \tilde{W}_h$, and $\|Q_h v\|_{0,\Gamma} \le C\|v\|_{0,\Gamma}$. We denote by P_h the L^2-projection on $\tilde{W}_h$ and note that $\|P_h v\|_{1,\Gamma} \le \|v\|_{1,\Gamma}$, $v \in H^1(\Gamma)$, see [Bra01]. In terms of the L^2-stability of Q_h, the approximation property of P_h and an inverse estimate, the $H_{00}^{\frac{1}{2}}$-stability of Q_h can be shown

$$\begin{aligned}\|Q_h v\|_{H_{00}^{\frac{1}{2}}(\Gamma)} &\le \|Q_h v - P_h v\|_{H_{00}^{\frac{1}{2}}(\Gamma)} + \|P_h v\|_{H_{00}^{\frac{1}{2}}(\Gamma)} \le C\left(\frac{1}{\sqrt{h_2}}\|Q_h v - P_h v\|_{0,\Gamma} + \|v\|_{H_{00}^{\frac{1}{2}}(\Gamma)}\right)\\ &\le C\left(\frac{1}{\sqrt{h_2}}\|v - P_h v\|_{0,\Gamma} + \|v\|_{H_{00}^{\frac{1}{2}}(\Gamma)}\right) \le C\|v\|_{H_{00}^{\frac{1}{2}}(\Gamma)}.\end{aligned}$$

Using the discrete harmonic extension on $S^p(\Omega_2, \mathcal{T}_{h_2})$, we obtain a uniform discrete inf-sup condition. The $H_{00}^{\frac{1}{2}}$-stability of Q_h guarantees the discrete inf-sup condition

$$\|\mu_h\|_{H^{-\frac{1}{2}}(\Gamma)} = \sup_{v\in H_{00}^{\frac{1}{2}}(\Gamma)\setminus\{0\}} \frac{\int_\Gamma \mu_h\, Q_h v\, ds}{\|v\|_{H_{00}^{\frac{1}{2}}(\Gamma)}} \le C \sup_{v\in H_{00}^{\frac{1}{2}}(\Gamma)\setminus\{0\}} \frac{\int_\Gamma \mu_h\, Q_h v\, ds}{\|Q_h v\|_{H_{00}^{\frac{1}{2}}(\Gamma)}}$$
$$\le C \sup_{w_h\in \tilde{W}_h\setminus\{0\}} \frac{\int_\Gamma \mu_h\, w_h\, ds}{\|w_h\|_{H_{00}^{\frac{1}{2}}(\Gamma)}} \le C \sup_{\tilde{w}_h\in S^p(\Omega_2,\mathcal{T}_{h_2})\setminus\{0\}} \frac{\int_\Gamma \mu_h\, \tilde{w}_h\, ds}{\|\tilde{w}_h\|_{1,\Omega_2}} \le C \sup_{\tilde{w}_h\in X_h\setminus\{0\}} \frac{b(\tilde{w}_h,\mu_h)}{\|\tilde{w}_h\|_{1,\Omega}},$$

where $\tilde{w}_h$ is the discrete harmonic extension of w_h to Ω_2 extended by zero on Ω_1. In terms of these preliminary considerations, we can apply [Bra01, Theorem III, 4.5] and get the following a priori bound for the discretization error

LEMMA 3.1. *The discrete variational problem* (3.1) *has a unique solution* (u_h, λ_h)*, and there exist two constants* c_1 *and* c_2 *independent of* h *such that*

$$\|u-u_h\|_{1,\Omega} + \|\lambda-\lambda_h\|_{H^{-\frac{1}{2}}(\Gamma)} \le c_1 \inf_{v_h\in X_h} \|u-v_h\|_{1,\Omega} + c_2 \inf_{\mu_h\in M_h} \|\lambda-\mu_h\|_{H^{-\frac{1}{2}}(\Gamma)}. \tag{3.2}$$

In a next step, we define another projection operator Q_h^* by

$$Q_h^* : H^{-\frac{1}{2}}(\Gamma) \longrightarrow M_h, \qquad \int_\Gamma Q_h^*\mu\, w_h\, ds = \int_\Gamma \mu\, w_h\, ds, \qquad w_h \in \tilde{W}_h$$

and note that $Q_h^*\mu = \mu$, $\mu \in M_h$, and $\|Q_h^*\mu\|_{0,\Gamma} \le C\|\mu\|_{0,\Gamma}$ An interpolation argument yields the $H_{00}^{\frac{1}{2}-s}$-stability, $0 \le s \le \frac{1}{2}$, of Q_h, and as a result, we find that Q_h^* is $H^{s-\frac{1}{2}}$-stable

$$\|Q_h^*\mu\|_{H^{s-\frac{1}{2}}(\Gamma)} = \sup_{w\in H_{00}^{\frac{1}{2}-s}(\Gamma)\setminus\{0\}} \frac{\langle Q_h^*\mu, w\rangle_\Gamma}{\|w\|_{H_{00}^{\frac{1}{2}-s}(\Gamma)}} = \sup_{w\in H_{00}^{\frac{1}{2}-s}(\Gamma)\setminus\{0\}} \frac{\langle Q_h^*\mu, Q_h w\rangle_\Gamma}{\|w\|_{H_{00}^{\frac{1}{2}-s}(\Gamma)}}$$
$$= \sup_{w\in H_{00}^{\frac{1}{2}-s}(\Gamma)\setminus\{0\}} \frac{\langle \mu, Q_h w\rangle_\Gamma}{\|w\|_{H_{00}^{\frac{1}{2}-s}(\Gamma)}} \le \|\mu\|_{H^{s-\frac{1}{2}}(\Gamma)}.$$

THEOREM 3.2. *Assume that* $u \in \prod_{k=1}^2 H^{r_k+1}(\Omega_k)$*, and* $\lambda \in \prod_{k=1}^N H^{r_2-\frac{1}{2}}(\gamma_k)$ *with* $r_1 \ge 0$ *and* $r_2 > \frac{1}{2}$*. Then, we have the following a priori estimate for the discretization error*

$$\|u-u_h\|_{1,\Omega} + \|\lambda-\lambda_h\|_{H^{-\frac{1}{2}}(\Gamma)} \le C(h_1^{2s_1}\|u\|_{s_1+1,\Omega_1}^2 + h_2^{2s_2}\|u\|_{s_2+1,\Omega_2}^2)^{\frac{1}{2}},$$

where $s_i := min(r_i, p)$*,* $i = 1, 2$*. If* $0 \le r_2 \le \frac{1}{2}$*, then we have*

$$\|u-u_h\|_{1,\Omega} + \|\lambda-\lambda_h\|_{H^{-\frac{1}{2}}(\Gamma)} \le C(h_1^{2s_1}\|u\|_{s_1+1,\Omega_1}^2 + h_2^{2s_2}\|u\|_{s_2+1,\Omega_2}^2 + h_2^{2r_2}\|\lambda\|_{H^{r_2-\frac{1}{2}}(\Gamma)}^2)^{\frac{1}{2}}.$$

Proof. The best approximation property of X_h is well-known, and we have

$$\inf_{u_h\in X_h} \|u-u_h\|_{1,\Omega} \le C(h_1^{2s_1}\|u\|_{s_1+1,\Omega_1}^2 + h_2^{2s_2}\|u\|_{s_2+1,\Omega_2}^2)^{\frac{1}{2}}, \quad u \in H^{r_1+1}(\Omega_1) \times H^{r_2+1}(\Omega_2).$$

To establish the best approximation error of M_h in the $H^{-\frac{1}{2}}$-norm on Γ, we work with Q_h^*. In a first step, we consider the case $r_2 > \frac{1}{2}$. The L^2-stability of Q_h^*, the best approximation property of $M_h(\gamma_l)$, see [Woh01], and the trace theorem yield for $\lambda \in \prod_{l=1}^N H^{r_2-\frac{1}{2}}(\gamma_l)$,

$$\|\lambda - Q_h^*\lambda\|^2_{H^{-\frac{1}{2}}(\Gamma)} := \sup_{v\in H_{00}^{\frac{1}{2}}(\Gamma)\backslash\{0\}} \frac{\langle \lambda - Q_h^*\lambda, v\rangle_\Gamma^2}{\|v\|^2_{H_{00}^{\frac{1}{2}}(\Gamma)}} \leq \sup_{v\in H_{00}^{\frac{1}{2}}(\Gamma)\backslash\{0\}} \frac{\|\lambda - Q_h^*\lambda\|^2_{0,\Gamma}\|v - Q_h v\|^2_{0,\Gamma}}{\|v\|^2_{H_{00}^{\frac{1}{2}}(\Gamma)}}$$

$$\leq C h_2 \|\lambda - Q_h^*\lambda\|^2_{0,\Gamma} \leq C h_2^{2s_2} \sum_{l=1}^N |\lambda|^2_{H^{s_2-\frac{1}{2}}(\gamma_l)} \leq C h_2^{2s_2} |u|^2_{s_2+1,\Omega_2}.$$

Now, we consider the case $0 \leq r_2 \leq \frac{1}{2}$. Using the $H^{r_2-\frac{1}{2}}$-stability of Q_h^*, we have

$$\begin{aligned}
\|\lambda - Q_h^*\lambda\|^2_{H^{-\frac{1}{2}}(\Gamma)} &:= \sup_{v\in H_{00}^{\frac{1}{2}}(\Gamma)\backslash\{0\}} \frac{\langle \lambda - Q_h^*\lambda, v\rangle_\Gamma^2}{\|v\|^2_{H_{00}^{\frac{1}{2}}(\Gamma)}} \\
&\leq \sup_{v\in H_{00}^{\frac{1}{2}}(\Gamma)\backslash\{0\}} \frac{\|\lambda - Q_h^*\lambda\|^2_{H^{r_2-\frac{1}{2}}(\Gamma)}\|v - Q_h v\|^2_{H_{00}^{\frac{1}{2}-r_2}(\Gamma)}}{\|v\|^2_{H_{00}^{\frac{1}{2}}(\Gamma)}} \\
&\leq C h_2^{2r_2} \|\lambda - Q_h^*\lambda\|^2_{H^{r_2-\frac{1}{2}}(\Gamma)} \leq C h_2^{2r_2} \|\lambda\|^2_{H^{r_2-\frac{1}{2}}(\Gamma)}.
\end{aligned}$$

Finally, the proof follows by using (3.2). ◻

REMARK 3.3. *Because of the corners at the interface, the given a priori estimate cannot be established for $r_2 \geq 1$ if we work with a Lagrange multiplier space which is directly defined on Γ. In that case an error term of $\mathcal{O}(h_2^{1-\epsilon})$, $\epsilon > 0$ occurs. This term is crucial in case of a smooth solution and quadratic finite elements.*

In the rest of this section, we consider the algebraic formulation of the saddle point problem (3.1) and apply a suitable modification to get a positive definite system on the product space. Here and in the following, we use the same notation for the vector representation of the solution and the solution as an element in X_h and M_h. The matrix A is the stiffness matrix associated with the bilinear form $a(\cdot,\cdot)$ on $X_h \times X_h$, and the matrices B and B^T are associated with the bilinear form $b(\cdot,\cdot)$ on $X_h \times M_h$. Then, the algebraic formulation of the saddle point problem is given by

$$\begin{pmatrix} A & B^T \\ B & 0 \end{pmatrix} \begin{pmatrix} u_h \\ \lambda_h \end{pmatrix} = \begin{pmatrix} f_h \\ g_h \end{pmatrix}, \tag{3.3}$$

where f_h and g_h are associated with the linear forms $f(\cdot)$ and $g(\cdot)$. Introducing $W_{0;h} := \prod_{l=1}^N W_{0;h}(\gamma_l)$, we define the mortar mapping $\Pi : X_h \longrightarrow W_{0;h} \subset X_h$ by

$$\int_\Gamma \Pi v\, \mu_h\, ds = \int_\Gamma [v]\, \mu_h\, ds, \quad \mu_h \in M_h$$

and denote its algebraic representation by W. We remark that W applied to an element in $(\ker B)_h$ is zero. Thus the non-zero blocks of W are associated with the slave and master nodes on the interface. Moreover in case of dual Lagrange multipliers, the mortar mapping can be locally evaluated and the non-zero blocks of W are sparse. We denote by E the matrix associated with the natural embedding of $W_{0;h}$ in X_h and by D the diagonal matrix with entries $d_{ii} := \int_\Gamma \varphi_i\, ds$, where φ_i are the nodal basis functions of $W_{0;h}$. It is easy to see that $DE^TW = B$ and $ED^{-1}B = W$. Static condensation of the Lagrange multiplier now yields

$$\lambda_h = D^{-1}E^T(f_h - Au_h). \tag{3.4}$$

This observation is the starting point for the modification of the algebraic formulation of the discrete saddle point problem (3.3). We use the equivalent form $\lambda_h = D^{-1}E^T(f_h - Au_h + AWu_h) - D^{-1}E^TAED^{-1}g_h$ of (3.4) to eliminate λ_h in (3.3). Shifting the terms in g_h and f_h to the right side yields

$$\begin{pmatrix} A & B^T \\ B & 0 \end{pmatrix} \begin{pmatrix} \mathrm{Id} \\ D^{-1}E^TA(W - \mathrm{Id}) \end{pmatrix} u_h = \begin{pmatrix} (\mathrm{Id} - W^T)f_h + W^TAED^{-1}g_h \\ g_h \end{pmatrix}. \quad (3.5)$$

We note that the jump in the trace enters now in both block components on the right side. The system (3.5) has more equations than unknowns. To obtain a positive definite system for u_h on the product space, we restrict the space of test functions. Assuming that the test function (v_h, μ_h) has the form $(v_h, D^{-1}E^TA(W - \mathrm{Id})v_h)$, we get

$$\tilde{A}u_h = \tilde{f}_h := (\mathrm{Id} - W^T)f_h + (2W^T - \mathrm{Id})AED^{-1}g_h, \quad (3.6)$$

where $\tilde{A} := (\mathrm{Id} - W^T)A(\mathrm{Id} - W) + W^TAW$. The matrix $\tilde{A}$ is symmetric and positive definite, see [Woh01].

LEMMA 3.4. *The saddle point problem* (3.1) *for* (u_h, λ_h) *and the positive definite system* (3.6) *for* u_h *together with the post-processing step* (3.4) *are equivalent.*

The proof follows by construction. We note that the matrix $\tilde{A}$ has exactly the same form as in a standard mortar problem with dual Lagrange multipliers, see [WK01]. The interface conditions enter only into the right side $\tilde{f}_h$ and do not influence the iterative solver. To solve the symmetric positive definite problem (3.6), we apply the modified multigrid approach proposed in [WK01] in combination with one local post-processing step of lower complexity. It is based on the decomposition of u_h in $u_h = (u_h - ED^{-1}g_h) + ED^{-1}g_h$.

REMARK 3.5. *Applying a Gauß–Seidel smoother, we do not have to carry out the post-process. The structure of the smoother guarantees that the weak discrete form of* (2.2) *is automatically satisfied within the multigrid approach.*

4. Numerical results. Here, we present some numerical examples illustrating the flexibility and efficiency of the mortar finite element method with dual Lagrange multipliers to treat interface problems. All our numerical examples are realized within the finite element toolbox ug, [BBJ+97]. We present the numerical results for various types of interface problems using linear and quadratic mortar finite elements. We denote by M_h^q and M_h^l the discontinuous dual Lagrange multiplier spaces for quadratic and linear finite elements, respectively, see [Woh01]. In the case of M_h^q, the basis functions are piecewise quadratic, whereas the basis functions of M_h^l are piecewise linear. The mortar finite element solutions associated with the different Lagrange multiplier spaces M_h^q and M_h^l are denoted by u_h^q and u_h^l, respectively. For all our numerical examples, we use uniform refinement. The error in the Lagrange multipliers is measured in a mesh-dependent L^2-norm

$$\|\lambda_h\|_h^2 := \sum_{e \in \mathcal{T}_\Gamma} h_e \|\lambda_h\|_{0;e}^2,$$

where h_e is the length of the edge e on the slave side. For our first example, we decompose $\Omega := (0,2) \times (0,1)$ into $\Omega_2 := (0.5, 1.5) \times (0.25, 0.75)$, and $\Omega_1 := \Omega \backslash \bar{\Omega}_2$, see the left picture of Figure 4.1. We note that Γ can be decomposed into four straight segments, γ_l, $1 \leq l \leq 4$.

The corner nodes of Ω_2 do not carry a degree of freedom for the Lagrange multiplier space. Here, we consider the problem (2.1)–(2.3) with

$$\alpha_1 := \begin{pmatrix} 2.5 & 0 \\ 0 & 1 \end{pmatrix}, \ \alpha_2 := \begin{pmatrix} 1 & 0 \\ 0 & 2.5 \end{pmatrix},$$

and $b_1(x,y) := x^2 + y^2 + xy$, $b_2(x,y) := 0$. The right-hand side, the interface conditions and Dirichlet boundary conditions are set such that one obtains the exact solution given by $u_1(x,y) := \sin(x^2+y)\exp(-(x-y)^2)$, and $u_2(x,y) := 1.5\exp(-(x-1)^2 - (y-0.5)^2)$.

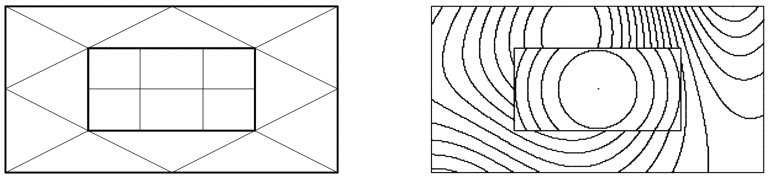

Fig. 4.1: Decomposition of the domain and initial triangulation (left) and isolines of the solution (right), Example 1

The isolines of the solution are given in the right picture of Figure 4.1, and the discretization errors are shown in Figure 4.2. The numerical results confirm the asymptotic rates as predicted by the theory. Having a decomposition where Γ is not a straight line does not influence the convergence rates. In contrast to mortar techniques with many subdomains and crosspoints, we do not have to reduce the dimension of the Lagrange multiplier space at the corners because of the inf-sup condition. The inf-sup condition is also satisfied for the higher dimensional space $\tilde{M}_h^l$ (or $\tilde{M}_h^q$), where $\tilde{M}_h^l$ (or $\tilde{M}_h^q$) is spanned by the biorthogonal basis functions (linear or quadratic) associated with all nodes including the corner nodes on the slave side. However, replacing the Lagrange multiplier space M_h^q by $\tilde{M}_h^q$ yields considerably worse numerical results for the discretization errors in the Lagrange multiplier. This is due to the fact that λ is not in $H^{\frac{1}{2}}(\Gamma)$, and this is crucial for quadratic finite elements, see Remark 3.3. In the right picture of Figure 4.2, we have given the errors in the weighted Lagrange multiplier norm using the space $\tilde{M}_h^q$ (not modified) and the space M_h^q (modified). Here, we see that if we work with the space $\tilde{M}_h^q$, the error in the weighted Lagrange multiplier norm is only of order $O(h)$.

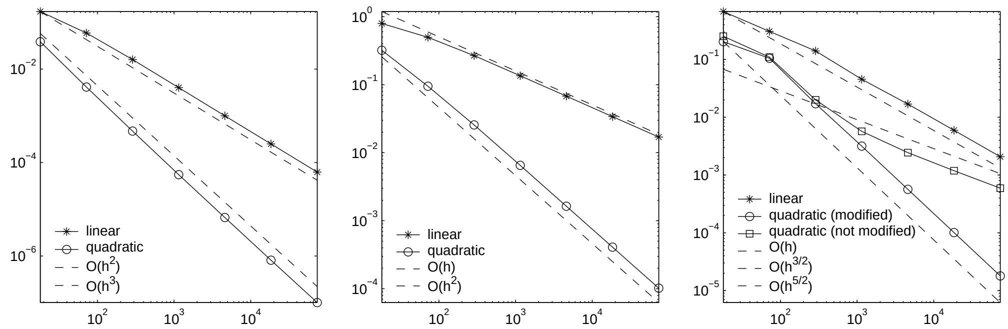

Fig. 4.2: Error plot versus number of elements, L^2-norm (left), H^1-norm (middle) and weighted Lagrange multiplier norm (right), Example 1

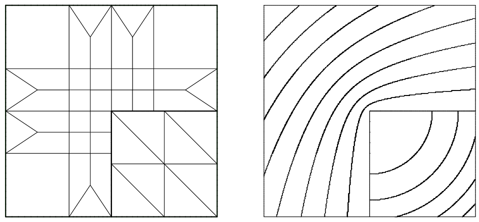

Fig. 4.3: Decomposition into two subdomains and initial triangulation (left) and isolines of the solution (right), Example 2

In our second example, we consider a problem with a corner singularity. Here, we decompose the unit square into two subdomains Ω_1 and Ω_2. The subdomain Ω_1 is a L-shape domain and $\Omega_2 := (0.5, 1) \times (0, 0.5)$, see the left picture of Figure 4.3. The initial triangulation does not match at the interface. The problem for this example is given by $-\Delta u = f$, and the exact solution is chosen as $u_1 := r^{2/3} \sin(\frac{2\phi}{3})$, and $u_2 := r^2$, where (r, ϕ) are the polar coordinates with origin shifted to $(0.5, 0.5)$. The isolines of the solution are shown in the right picture of Figure 4.3. Here, the solution is not piecewise H^2-regular, and asymptotically we cannot expect the same order of convergence as in the first example. The errors in the L^2-, H^1- and the weighted Lagrange multiplier norms are given in Table 4.1. Here we use lowest order finite elements. Asymptotically, we expect an order $h^{2/3}$ for the H^1-norm which can be observed. We note that the convergence rates are considerably better in the beginning. In contrast to the first example, the Lagrange multiplier does not show a better asymptotic convergence rate. Asymptotically, we obtain the same convergence rate as in the H^1-norm. This is due to the concentration of the error at the point $(0.5, 0.5)$ which is located on the interface. Better convergence rates in the Lagrange multiplier norm can only be observed if the solution has no singularity at the interface.

Table 4.1

Discretization errors in the L^2-, H^1- and weighted Lagrange multiplier norm, Example 2

level	# elem.	$\|\|u - u_h^l\|\|_0$	ratio	$\|\|u - u_h^l\|\|_1$	ratio	$\|\|\lambda - \lambda_h^l\|\|_h$	ratio
0	41	3.325808e-02		1.370511e-01		1.667159e-02	
1	164	8.446641e-03	3.9374	7.408534e-02	1.8499	4.399131e-03	3.7897
2	656	2.122112e-03	3.9803	4.111530e-02	1.8019	1.584474e-03	2.7764
3	2624	5.335827e-04	3.9771	2.343380e-02	1.7545	7.218470e-04	2.1950
4	10496	1.348615e-04	3.9565	1.369342e-02	1.7113	3.889129e-04	1.8561
5	41984	3.434135e-05	3.9271	8.173967e-03	1.6752	2.289971e-04	1.6983
6	167936	8.837528e-06	3.8859	4.961475e-03	1.6475	1.403140e-04	1.6320
7	671744	2.307613e-06	3.8297	3.048681e-03	1.6274	8.741203e-05	1.6052

In our third example, the domain, the problem and the exact solution are taken from [AL02]. For this example, the domain $\Omega := (-1, 1) \times (-1, 1)$ is decomposed into two subdomains Ω_1 and Ω_2, where Ω_2 is a circle with radius 0.5 centered at the origin, and $\Omega_1 := \Omega \backslash \bar{\Omega}_2$, see the left picture of Figure 4.4. We remark that, in this example, the interface cannot be decomposed into straight lines. In addition to the analysis given in Section 3, the polygonal approximation of Γ has to be taken into account. Here, $b_1(x, y) := 0$, $b_2(x, y) := 0$, $\alpha_1 := 0.1\, I_2$, and $\alpha_2 := (x^2 + y^2 + 1)\, I_2$ in (2.1)–(2.3), where I_2 is the 2×2 identity matrix. The exact solution is given as

$$u_1 := -\frac{41}{16} + 5\,\left(x^2 + y^2\right)^2 + 10\,x^2 + 10\,y^2 + 10\,C \ln\left(2\,\sqrt{x^2 + y^2}\right), \quad \text{and} \quad u_2 := x^2 + y^2.$$

The jump of the trace and of the flux across the interface Γ are computed as $[u] = 0$, and $[u]_n = -2C$, and we have set $C := 10$. The right-hand side and the Dirichlet boundary condition on $\partial\Omega$ are computed by using the given exact solution. Here too, we use only the lowest order finite elements. The discretization errors in the L^2-, H^1- and the weighted Lagrange multiplier norm (weighted L^2-norm) for the linear finite elements are given in the right picture of Figure 4.4. As before, we observe numerically the predicted convergence rates.

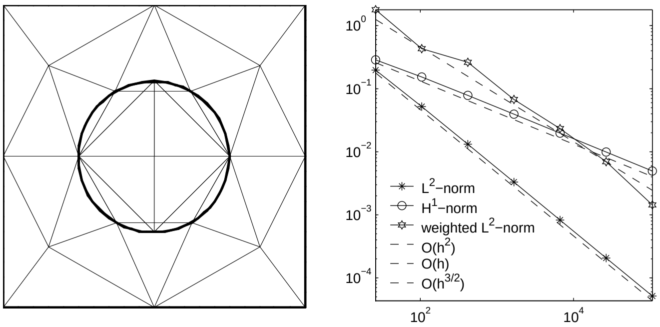

Fig. 4.4: Decomposition into two subdomains and initial triangulation (left) and error plot versus number of elements (right), Example 3

In our last example, we consider a problem of linear elasticity. We remark that the theoretical results can easily be generalized to this case. For this example, we take the domain $\Omega := (-1,1) \times (-1,1)$ decomposed into an upper and a lower triangle, Ω_1 and Ω_2, respectively, with the common interface $\Gamma := \{(x,x) : -1 \leq x \leq 1\}$, see the left picture of Figure 4.5.

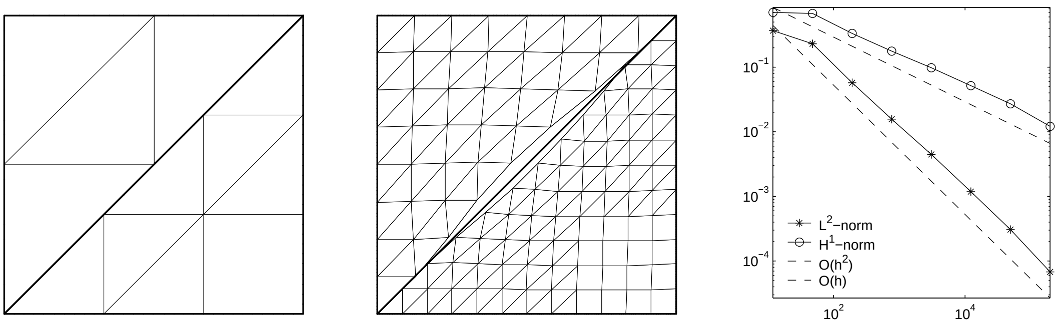

Fig. 4.5: Decomposition into two subdomains and initial triangulation (left), distorted grid on level 2 (middle) and error plot versus number of elements (right), Example 4

We have used homogeneous Dirichlet boundary condition on $\partial\Omega$, and the jump of the flux and the jump of the trace are given by $g_N := (0,0)^T$ and $g_D := (g(x),0)^T$, respectively. Here, $g(x)$ is defined by

$$g(x) := \begin{cases} 0 & \text{if } x \in [-1,-0.6] \cup [0.6,1] \\ 0.5(x+0.6)(x-0.6) & \text{if } x \in (-0.6,0.6). \end{cases}$$

This leads to a crack on the interface Γ, which is shown in the middle picture of Figure 4.5. Young's modulus E and Poisson ratio ν are chosen to be 71GPa and 0.35 for the lower triangle, and 35GPa and 0.17 for the upper triangle, respectively. We apply the body force of 4MN on Ω along both directions. We do not have an analytical solution for this problem. To obtain the discretization error, we compute a reference solution on a very fine triangulation with meshsize h_{ref}, and compute an approximation of the error by comparing u_{ref} with u_h. We use the same u_{ref} for all refinement levels. On level 7 (starting from level 0), we have $h = 2h_{\text{ref}}$. As a result, we observe numerically better convergence rate in the last refinement step. There is a weak singularity in the stress at the opening of the crack. Thus, we apply only linear finite elements. The discretization errors are given in the right picture of Figure 4.5. This shows that we get an almost optimal order of convergence even in this case.

REFERENCES

[AL02] L. Adams and Z. Li. The immersed interface/multigrid methods for interface problems. *SIAM J. Sci. Comp.*, 24:463–479, 2002.

[Bab70] I. Babuška. The finite element method for elliptic equations with discontinuous coefficients. *Computing*, 5:207–213, 1970.

[BBJ+97] P. Bastian, K. Birken, K. Johannsen, S. Lang, N. Neuß, H. Rentz–Reichert, and C. Wieners. UG – a flexible software toolbox for solving partial differential equations. *Computing and Visualization in Science*, 1:27–40, 1997.

[Bel99] F. Ben Belgacem. The mortar finite element method with Lagrange multipliers. *Numer. Math.*, 84:173–197, 1999.

[BHS03] R. Becker, P. Hansbo, and R. Stenberg. A finite element method for domain decomposition with non-matching grids. M^2AN, 37:209–225, 2003.

[BK96] J.H. Bramble and J.T. King. A finite element method for interface problems in domains with smooth boundaries and interfaces. *Adv. Comput. Math.*, 6:109–138, 1996.

[BMP93] C. Bernardi, Y. Maday, and A.T. Patera. Domain decomposition by the mortar element method. In H. Kaper et al., editor, *In: Asymptotic and numerical methods for partial differential equations with critical parameters*, pages 269–286. Reidel, Dordrecht, 1993.

[BMP94] C. Bernardi, Y. Maday, and A.T. Patera. A new nonconforming approach to domain decomposition: the mortar element method. In H. Brezzi et al., editor, *In: Nonlinear partial differential equations and their applications*, pages 13–51. Paris, 1994.

[Bra01] D. Braess. *Finite Elements. Theory, fast solver, and applications in solid mechanics.* Cambridge Univ. Press, Second Edition, 2001.

[CG98] Y. Cao and M.D. Gunzburger. Least-squares finite element approximations to solutions of interface problems. *SIAM J. Numer. Anal.*, 35:393–405, 1998.

[CZ98] Z. Chen and J. Zou. Finite element methods and their convergence for elliptic and parabolic interface problems. *Numer. Math.*, 79:175–202, 1998.

[HH02] A. Hansbo and P. Hansbo. An unfitted finite element method, based on Nitsche's method, for elliptic interface problems. *Comput. Methods Appl. Mech. Engrg.*, 191:5537–5552, 2002.

[HN03] B. Heinrich and S. Nicaise. Nitsche mortar finite element method for transmission problems with singularities. *IMA J. Numer. Anal.*, 23:331–358, 2003.

[HZ02] J. Huang and J. Zou. Some new a priori estimates for second-order elliptic and parabolic interface problems. *J. Differ. Equations*, 184:570–586, 2002.

[Li98a] Z. Li. A fast iterative algorithm for elliptic interface problems. *SIAM. J. Numer. Anal.*, 35:230–254, 1998.

[Li98b] Z. Li. The immersed interface method using a finite element formulation. *Appl. Numer. Math.*, 27:253–267, 1998.

[LL94] R.J. LeVeque and Z.L. Li. The immersed interface method for elliptic equations with discontinuous coefficients and singular sources. *SIAM. J. Numer. Anal.*, 31:1019–1044, 1994.

[WB00] A. Wiegmann and K.P. Bube. The explicit-jump immersed interface method: Finite difference methods for pdes with piecewise smooth solutions. *SIAM J. Numer. Anal.*, 37:827–862, 2000.

[WK01] B.I. Wohlmuth and R.H. Krause. Multigrid methods based on the unconstrained product space arising from mortar finite element discretizations. *SIAM J. Numer. Anal.*, 39:192–213, 2001.

[Woh01] B.I. Wohlmuth. *Discretization Methods and Iterative Solvers Based on Domain Decomposition*, volume 17 of *LNCS*. Springer Heidelberg, 2001.

[XZ98] J. Xu and J. Zou. Some non-overlapping domain decomposition methods. *SIAM Review*, 40:857–914, 1998.